PHYSICAL REVIEW A **95**, 042512 (2017)

Low-energy $E0$ transition between the components of the ground-state doublet in the muonic atom ^{229}Th

E. V. Tkalya*

Skobeltsyn Institute of Nuclear Physics Lomonosov Moscow State University, Leninskie gory, Moscow 119991, Russia;
Nuclear Safety Institute of Russia Academy of Sciences, Bol'shaya Tulskaya 52, Moscow 115191, Russia;
and National Research Nuclear University Moscow Engineering Physics Institute, 115409, Kashirskoe shosse 31, Moscow, Russia

(Received 5 December 2016; published 20 April 2017)

The probability of the $E0$ transition between the components of the magnetic hyperfine (MHF) structure of the ground $5/2^+(0.0)$ and the low-energy $3/2^+(7.8 \pm 0.5$ eV) levels is calculated in the muonic atom $(\mu^-_{1S_{1/2}}{}^{229}\mathrm{Th})^*$. [The MHF splitting taking into account the Bohr-Weisscopf effect and the mixing of the $F = 2$ sublevels was found earlier in the paper E. V. Tkalya, Phys. Rev. A **94**, 012510 (2016)] The mean-square charge radius of the isomeric state in ^{229}Th is estimated from the data for the $3/2^+(0.0)$ state of the ^{223,227}Ra nuclei and the $5/2^+(0.0)$ state of the ^{221,229}Ra nuclei. The resulting $E0$ transition probability is found to be anomalously small in comparison to the known value for the $0^+ \to 0^+$ nuclear transitions, which is explained by the similarity between the mean-square charge radii of the ground and low-energy isomeric states in ^{229}Th.

DOI: 10.1103/PhysRevA.95.042512

I. INTRODUCTION

The ^{229}Th nucleus has the anomalously low-energy level $J^\pi(E) = 3/2^+(7.8 \pm 0.5\,\mathrm{eV})$ [1,2]. The "optical" character of the magnetic dipole ($M1$) transition between the ground state, $5/2^+(0.0)$, and the first excited state of the ^{229}Th nucleus was first noticed by the authors of Refs. [3,4]. Direct confirmation that this isomeric level lies in the range 6.3–18.3 eV, has been given recently by the authors of Ref. [5]. The most common restrictions on the parameters of the $3/2^+$ level were established in Refs. [6,7].

From the point of view of the nuclear spectroscopy this is an absolutely unique situation. The isomeric transition $3/2^+(7.8 \pm 0.5$ eV$) \to 5/2^+(0.0)$ (with energy close to the optical range) makes the ^{229}Th nucleus suitable for the study of various new physical phenomena: the cooperative spontaneous emission [8] of the excited ^{229}Th nuclei, the "nuclear light" [9,10] and the electronic bridge [11–13], the α decay of the isomeric state [14], the Mößbauer effect in the optical range [15], tests of the variation of the fine-structure constant [16] and the strong interaction parameter [17–20], a check of the exponentiality of the decay law [21], and others. A "nuclear clock" [22–25] and a nuclear laser (or gamma ray laser) in the optical range [15,26] are of particular interest. These devices, if they can be created, will have great potential for applications. That is why the intensive experimental study of this transition and its properties are currently under way in several research teams [1,5,6,23–25,27–33].

With regard to the characteristics of the low-lying isomeric level $3/2^+(7.8 \pm 0.5$ eV), at the present time we have theoretical estimations of its magnetic moment [34], the quadrupole moment [35], and the nuclear matrix element of the transition to the ground state [7,34]. All these parameters are obtained by the conventional methods of nuclear spectroscopy.

On the other hand, it is well known that muonic atoms are a powerful tool for investigating the nuclear forces and structure. The muon mass is about 200 times that of the electron. That makes the Bohr radius for the muonic atom a_{B_μ} 200 times smaller. In addition, the orbital electrons practically do not screen the nucleus for the muon in the $1S_{1/2}$ state. And the system "nucleus + muon" resembles a hydrogen-like ion with the characteristic size a_{B_μ}/Z (Z is the nucleus charge), which is comparable to the size of the nucleus itself. Therefore the muon is sensitive to the distribution of currents and charges in the nucleus. This allows us to study the nuclear properties with much higher accuracy.

The measurement of the nucleus mean-square charge radius in muonic atoms is a well-known example of such research. The mean-square charge radius is an important parameter, directly related to the nuclear forces and nuclear structure. Currently the problem of the charge radius of the proton [36–41] and the deutron [42] is studied intensively by using muonic atoms. This problem is known in the scientific literature as "the proton (deutron) radius puzzle." The fact is that the Lamb shift and transitions between the components of the hyperfine structure of the $2S_{1/2}$ and $2P_{1/2,3/2}$ levels in muonic atoms are extraordinarily sensitive to the root mean-square charge radius of nuclei. As a consequence, one can extract the required data on the nuclear structure directly by measuring the Lamb shift and the energy of these transitions. However, another approach is also possible.

In this paper, we show that there is a fundamental possibility to determine the unknown mean-square charge radius of the ^{229}Th nucleus in the $3/2^+(7.8 \pm 0.5$ eV) state in the muonic atom. In contrast to the measurements of the energy of the $2P_{1/2,3/2} - 2S_{1/2}$ and $2P_{1/2,3/2} - 1S_{1/2}$ transitions, this can be done by measuring the $E0$ transition probability between components of the magnetic hyperfine structure of the ground-state doublet in $(\mu^-_{1S_{1/2}}{}^{229}\mathrm{Th})^*$ [43]. This $E0$ transition occurs after the muon reached the $1S_{1/2}$ state and all the fast relaxation processes in the electron shell of the atom ended.

II. $E0$ TRANSITION IN MUONIC ATOM

The $E0$ component is always present in the nuclear $J^\pi \to J^\pi$ transitions, i.e., in transitions between states with

*tkalya@srd.sinp.msu.ru

 ©2017 American Physical Society

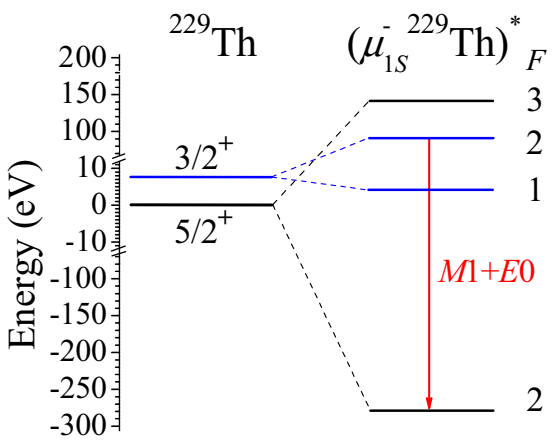

FIG. 1. The magnetic hyperfine structure of the ^{229}Th ground-state doublet in muonic atom, Ref. [43], which takes into account the mixing of sublevels, the distribution of the magnetic dipole moment over the nuclear volume [52], and the penetration effect [53].

the same spin and parity. Here we will investigate the $E0$ transition, which links the states with different spins. This is somewhat unusual. The possible occurrence of the $E0$ component at the transition in Fig. 1 is an interesting feature of the muonic atom $(\mu^-_{1S_{1/2}}\ ^{229}\mathrm{Th})^*$. In this atom the magnetic dipole interaction between the orbital muon in the $1S_{1/2}$ shell and the nucleus in the ground and isomeric states leads to a number of interesting effects: a partial inversion of levels, the spontaneous decay of the ground state to the isomeric state, the mixing of the states with the same quantum number F ($F = J \pm 1/2$) [44], and the existence of the $E0$ component in the transition between the $F = 2$ states [43].

It is well known that the $E0$ transition is a signature of a mixing of configurations with different mean-square charge radii [45]. This is also true for the transition in Fig. 1. In the even-odd nucleus ^{229}Th, which consists of 90 protons and 139 neutrons, the first two levels are characterized by the state of the unpaired neutron in the Nilsson model [46]: $K^\pi[Nn_Z\Lambda] = 5/2^+[633]$ for the ground state, and $3/2^+[631]$ for the first excited state [35]. The unpaired neutron in the states $3/2^+[631]$ and $5/2^+[633]$ polarizes the core, namely, the ^{228}Th nucleus a little bit differently. This leads to a small difference in the mean-square charge radii and provides the $E0$ transition in the muonic atom $(\mu^-_{1S_{1/2}}\ ^{229}\mathrm{Th})^*$.

Since the radiation of the $E0$ photon is not possible, such a nuclear transition occurs with the transfer of excitation energy to the atomic shell, described by the second-order diagram in the the framework of the perturbation theory for the quantum electrodynamics. A corresponding process is called the internal conversion (IC). $E0$ Transitions are usually observed in even-even nuclei between the 0^+ states [47], when transitions of other multipoles are forbidden. Internal conversion in such transitions takes place mainly due to the inner shells of atoms because the characteristic energies of the transitions are of about hundreds keV to several MeV. Corresponding atomic matrix elements are calculated and tabulated in Refs. [48–50].

The energy of the $E0$ transition in ^{229}Th, computed with the currently accepted values for the intrinsic g factor g_K of the $3/2^+[631]$ rotational band and the nuclear reduced probability $B(M1; 3/2^+ \to 5/2^+)$ of the interband transition between the ground and isomeric states is about 370 eV. Large uncertainties in the values of g_K and $B(M1; 3/2^+ \to 5/2^+)$ lead to the following range for the $E0$ transition energies $\omega_{E0} = 370^{+30}_{-140}$ eV [43].

The internal-conversion process for the $E0$ (370 eV) transition in $(\mu^-_{1S_{1/2}}\ ^{229}\mathrm{Th})^*$ occurs through the $5S_{1/2}$, $6S_{1/2}$, $7S_{1/2}$, $5P_{1/2}$, and $6P_{1/2}$ shells. However, $E0$ transitions with very low energies have not been considered, and the electronic factors $\Omega_{O_{I,II}}$, $\Omega_{P_{I,II}}$, Ω_{Q_I} for them have not been calculated and tabulated [49,51]. Therefore, here we present the necessary calculations including the electronic parts.

III. PROBABILITY OF $E0$ INTERNAL CONVERSION

The probability of the $E0$ internal electronic conversion is calculated from Fermi's golden rule

$$W_{E0} = 2\pi |\langle \Phi_f | \hat{H}_{\rm int} | \Phi_i \rangle|^2 \rho_e \,, \tag{1}$$

where $\Phi_{i,f}$ are the wave functions of the initial and final states, ρ_e is the density of the electron final state: $\rho_e = (2\pi)^{-3} d^3p/dE = (2\pi)^{-3} mpd\Omega_e$, m is the electron mass, $p = \sqrt{2mE}$ is the electron momentum in the final state, i.e., the momentum of the conversion electron which has the energy E (the adopted system of units is $\hbar = c = 1$).

The Hamiltonian of the interaction between the electron and the "nuclei + muon" ion has the form

$$\hat{H}_{\rm int} = \hat{H}^{(p)}_{\rm int} + \hat{H}^{(\mu)}_{\rm int} \,, \tag{2}$$

where

$$\hat{H}^{(p)}_{\rm int} = \sum_{p=1}^{Z} \frac{-e^2}{|\mathbf{R}_p - \mathbf{r}_e|} \tag{3}$$

is the Hamiltonian of the interaction between electron and nuclei protons (Z is the nuclei charge), and

$$\hat{H}^{(\mu)}_{\rm int} = \frac{e^2}{|\mathbf{r}_\mu - \mathbf{r}_e|} \tag{4}$$

stands for the interaction between the electron and the muon (in the $1S_{1/2}$ shell), $\mathbf{R}_p$, $\mathbf{r}_\mu$, and $\mathbf{r}_e$ are the radius vectors of the pth proton, muon, and electron, respectively.

The wave functions $\Phi_{i,f}$ of mixed $F = 2$ states (shown in Fig. 1) have the form [43]

$$\begin{aligned} \Phi_i(\{\mathbf{R}\},\mathbf{r}_\mu,\mathbf{r}_e) &= \phi_i(\{\mathbf{R}\},\mathbf{r}_\mu)\psi_i(\mathbf{r}_e), \\ \Phi_f(\{\mathbf{R}\},\mathbf{r}_\mu,\mathbf{r}_e) &= \phi_f(\{\mathbf{R}\},\mathbf{r}_\mu)\psi_f(\mathbf{r}_e). \end{aligned} \tag{5}$$

where $\psi_i(\mathbf{r}_e)$, $\psi_f(\mathbf{r}_e)$ are the electron wave function in the atomic and continuum state, respectively, while $\phi_{i,f}(\{\mathbf{R}\},\mathbf{r}_\mu)$ are the muon-nucleus wave functions

$$\begin{aligned} \phi_i(\{\mathbf{R}\},\mathbf{r}_\mu) &= \sqrt{1-b^2}\Psi_i(\{\mathbf{R}\})\varphi_i(\mathbf{r}_\mu) + b\Psi_f(\{\mathbf{R}\})\varphi_f(\mathbf{r}_\mu), \\ \phi_f(\{\mathbf{R}\},\mathbf{r}_\mu) &= \sqrt{1-b^2}\Psi_f(\{\mathbf{R}\})\varphi_f(\mathbf{r}_\mu) - b\Psi_i(\{\mathbf{R}\})\varphi_i(\mathbf{r}_\mu). \end{aligned} \tag{6}$$

Here $\Psi(\{\mathbf{R}\})$ and $\varphi(\mathbf{r}_\mu)$ are the wave functions of the nucleus and the muon.

In Eqs. (5) to (6) $\{\mathbf{R}\} = \{\mathbf{R}_n, \mathbf{R}_p\}$ is a set of radius vectors of neutrons (n), and protons (p), for the nucleus. The value of the mixing coefficient $b \simeq 0.47$ for the muonic atom $(\mu^-_{1S_{1/2}}{}^{229}\mathrm{Th})^*$ in Eq. (6) was found in Ref. [43] by taking into account: (a) the dynamic effect of the nuclear volume [53] (or what is the same, the penetration effect [54]) for the interaction of the muon and nuclear currents, and (b) the distribution of the magnetic dipole moment over the nuclear volume for the static interaction of the muon with a magnetic field created by the nucleus in the ground and isomeric states (the Bohr-Weisskopf effect [52]).

In our case $\Psi_i(\{\mathbf{R}\})$ is the isomeric state $3/2^+(7.8\ \mathrm{eV})$ of the ^{229}Th nucleus, and $\Psi_f(\{\mathbf{R}\})$ is the ground state $5/2^+(0.0)$. The muon wave functions $\varphi_{i,f}(\mathbf{r}_\mu)$ describes the muon at the $1S_{1/2}$ shell with different projections of the muon spin.

For the calculation we shall use the standard multipole expansion

$$\frac{1}{|\mathbf{r}_< - \mathbf{r}_>|} = \frac{4\pi}{r_>} \sum_{L,M} \frac{1}{2L+1} \left(\frac{r_<}{r_>}\right)^L Y^*_{LM}(\Omega_>) Y_{LM}(\Omega_<), \tag{7}$$

where $\mathbf{r}_<$ is a smaller vector and $\mathbf{r}_>$ is a bigger vector. In the simplest case of the $E0$ internal conversion we get $1/|\mathbf{r}_< - \mathbf{r}_>| \to 1/r_>$.

The matrix element for the Hamiltonian (3) is given by

$$\begin{aligned}\langle \Phi_f | \hat{H}^{(p)}_{\mathrm{int}} | \Phi_i \rangle = \sum_{p=1}^{Z} \int_0^\infty d^3 r_\mu \int_0^\infty d^3\{R\} \\ \times \phi^*_f(\{\mathbf{R}\}, \mathbf{r}_\mu) \phi_i(\{\mathbf{R}\}, \mathbf{r}_\mu) \\ \times \left[\int_{R_p}^\infty d^3 r_e \psi^*_f(\mathbf{r}_e) \frac{-e^2}{r_e} \psi_i(\mathbf{r}_e) \right. \\ \left. + \int_0^{R_p} d^3 r_e \psi^*_f(\mathbf{r}_e) \frac{-e^2}{R_p} \psi_i(\mathbf{r}_e) \right].\end{aligned} \tag{8}$$

(Here and below, the notation $\int_a^b d^3x$ means $\int_0^{2\pi} d\varphi \int_0^\pi \sin(\theta) d\theta \int_a^b x^2 dx$.)

In Eq. (8) we make the substitution $\int_R^\infty d^3 r_e \to \int_0^\infty d^3 r_e - \int_0^R d^3 r_e$. The integral $\int_0^\infty d^3 r_e \psi^*_f(\mathbf{r}_e)(-e^2/r_e)\psi_i(\mathbf{r}_e)$ is a constant that can be taken outside the integration. In this case the remaining integrals give zero

$$\int_0^\infty d^3 r_\mu \int_0^\infty d^3\{R\} \phi^*_f(\{\mathbf{R}\}, \mathbf{r}_\mu) \phi(\{\mathbf{R}\}, \mathbf{r}_\mu) = 0$$

since all the wave functions are orthonormal: $\int_0^\infty d^3\{R\} \Psi^*_f(\{\mathbf{R}\}) \Psi_i(\{\mathbf{R}\}) = \delta_{if}$ and $\int_0^\infty d^3 r_\mu \varphi^*_f(\mathbf{r}_\mu) \varphi_i(\mathbf{r}_\mu) = \delta_{if}$, where δ_{if} is the Kronecker symbol.

As a result, the expression in square brackets in Eq. (8) is simplified and one gets

$$\begin{aligned}\langle \Phi_f | \hat{H}^{(p)}_{\mathrm{int}} | \Phi_i \rangle = \sum_{p=1}^{Z} \int_0^\infty d^3 r_\mu \int_0^\infty d^3\{R\} \\ \times \phi^*_f(\{\mathbf{R}\}, \mathbf{r}_\mu) \phi_i(\{\mathbf{R}\}, \mathbf{r}_\mu) \\ \times \int_0^{R_p} d^3 r_e \psi^*_f(\mathbf{r}_e) \left(\frac{-e^2}{R_p} - \frac{-e^2}{r_e} \right) \psi_i(\mathbf{r}_e).\end{aligned} \tag{9}$$

The upper limit of the integrals in Eq. (9) satisfies the condition $R_p \leqslant R_0 = 1.2A^{1/3}$ fm, where R_0 is the radius of the nucleus with the atomic number A. Therefore, we can take the approximate values of the electron wave functions $\psi_{i,f}(\mathbf{r}_e)$ inside the nucleus: $\psi_{i,f}(0) \simeq c_{i,f}/\sqrt{4\pi}$ [53]. Here $c_i = g_{nS_{1/2}}(0)/a_B^{3/2}$ for the $nS_{1/2}$ binding electron states normalized by the condition $\int_0^\infty dr_e r_e^2 [g^2(r_e) + f^2(r_e)] = a_B^3$, and $c_f = g_{S_{1/2}}(0)$ for the continuum states. The wave function of the final state has the asymptotic behavior of a plane wave plus a convergent spherical wave. The functions $g(r_e)$ and $f(r_e)$ are the large and small components of the Dirac bispinor, a_B is the Bohr radius. Similarly, for the $P_{1/2}$ states we have $c_i = f_{nP_{1/2}}(0)/a_B^{3/2}$ for the $nP_{1/2}$ binding electron state, and $c_f = f_{P_{1/2}}(0)$ for the continuum states. Other electronic states have close to zero amplitude of the wave functions at the nucleus and do not contribute to the probability of the $E0$ internal conversion. Now the integrals over the electron coordinate r_e in Eq. (9) can be easily calculated: $\int_0^R d^3 r_e(\ldots) = -e^2 c_i c^*_f(-R^2/6)$, and we finally obtain

$$\langle \Phi_f | \hat{H}^{(p)}_{\mathrm{int}} | \Phi_i \rangle = -e^2 \frac{c_i c^*_f}{6} b\sqrt{1-b^2} (\langle R^2 \rangle_i - \langle R^2 \rangle_f), \tag{10}$$

where

$$\langle R^2 \rangle_{i(f)} = \sum_{p=1}^{Z} \int d^3\{R\}\, \Psi^*_{i(f)}(\{\mathbf{R}\}) R_p^2 \Psi_{i(f)}(\{\mathbf{R}\}) \tag{11}$$

is the mean-square charge radius of the nucleus in the state $i(f)$.

The same calculation for the matrix element of the electron–muon Hamiltonian (4) leads to zero

$$\langle \Phi_f | \hat{H}^{(\mu)}_{\mathrm{int}} | \Phi_i \rangle = e^2 \frac{c_i c^*_f}{6} b\sqrt{1-b^2} \left(\langle r^2_\mu \rangle_i - \langle r^2_\mu \rangle_f \right) = 0, \tag{12}$$

since the muon remains in the $1S_{1/2}$ state in the considered $E0$ transition, and therefore $\langle r^2_\mu \rangle_i = \langle r^2_\mu \rangle_f$. [We recall that the muon wave functions $\varphi_i(\mathbf{r}_\mu)$ and $\varphi_f(\mathbf{r}_\mu)$ differ only by the spin projection.]

Substituting Eq. (10) to Eq. (1) and integrating over the angles $d\Omega_e$ we obtain for the probability of the $E0$ internal conversion

$$W_{E0} = \frac{e^4 m}{36\pi} b^2 (1-b^2) (\langle R^2 \rangle_i - \langle R^2 \rangle_f)^2 |c_i|^2 |c_f|^2 p. \tag{13}$$

For the $E0$ transition in the in muonic atom $(\mu^-_{1S_{1/2}}{}^{229}\mathrm{Th})^*$ we have

$$\begin{aligned}W_{E0} = \frac{e^4 m}{36\pi} b^2 (1-b^2) (\langle R^2 \rangle_{3/2^+} - \langle R^2 \rangle_{5/2^+})^2 \\ \times 2 \sum_n \left(\frac{|g_{nS_{1/2}}(0)|^2}{a_B^3} |g_{S_{1/2}}(0)|^2 p_{S_{1/2}} \right. \\ \left. + \frac{|f_{nP_{1/2}}(0)|^2}{a_B^3} |f_{P_{1/2}}(0)|^2 p_{P_{1/2}} \right).\end{aligned} \tag{14}$$

(The factor of 2 on the right hand side is accounted for by two electrons in each electron shell.) The electron momentum in the final state is $p_{S_{1/2}(P_{1/2})} = \sqrt{2m(\omega_{E0} - E_{nS_{1/2}(nP_{1/2})})}$, where $E_{nS_{1/2}(nP_{1/2})}$ is the binding energy of the $nS_{1/2}(nP_{1/2})$ subshell.

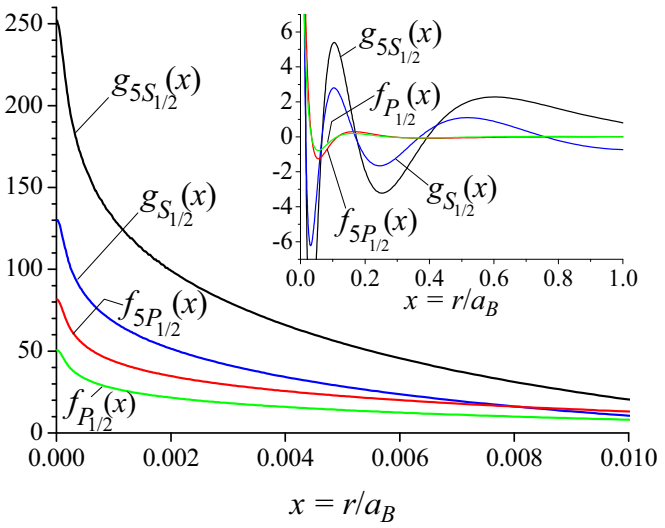

FIG. 2. The electron continuum wave functions $g_{S_{1/2}}$ and $f_{P_{1/2}}$ and the binding electron states $g_{5S_{1/2}}$ and $f_{5P_{1/2}}$ for the $E0$ internal conversion in the Ac atom.

For $\omega_{E0} = 370$ eV $n = 5$, 6, and 7 for the $nS_{1/2}$ states and $n = 5$, and 6 for the $nP_{1/2}$ states.

The muon in $(\mu^-_{1S_{1/2}}{}^{229}\text{Th})^*$ is located practically inside the thorium nucleus. Electronic shell experiences the system "muon + Thorium nucleus" as the Actinium nucleus of charge 89. The calculation of the electron wave functions in the shell of the Ac atom was performed using the code developed by the authors of Ref. [55] on the basis of the codes [56], and then advanced in Ref. [11]. The results of the electron calculations are quoted in Fig. 2 and Table I. The precise calculations of the $g_i(0)$ and $f_i(0)$ values within the density functional method by the code [57,58] gave practically the same result.

IV. NUCLEAR MATRIX ELEMENT

To calculate the probability of the $E0$ transition we need to know the values of $\langle R^2\rangle_{3/2^+}$, and $\langle R^2\rangle_{5/2^+}$. There are no experimental data about the magnitude of the mean-square charge radius of the low-lying isomeric state in the ^{229}Th nucleus. Therefore, as an estimation of the difference $\langle R^2\rangle_{3/2^+} - \langle R^2\rangle_{5/2^+}$, we use the available experimental data [59] for the mean-square charge radius of the states $5/2^+[633]$ and $3/2^+[631]$ in the neighboring isotopes of radium (see Fig. 3).

TABLE I. The amplitudes of the wave functions at the nucleus ($r_e = 0$).

Initial state	$g_i(0)$	Final state	$g_f(0)$
$5S_{1/2}$	252	$S_{1/2}$	129
$6S_{1/2}$	112	$S_{1/2}$	174
$7S_{1/2}$	35	$S_{1/2}$	178
Initial state	$f_i(0)$	Final state	$f_f(0)$
$5P_{1/2}$	82	$P_{1/2}$	51
$6P_{1/2}$	34	$P_{1/2}$	62

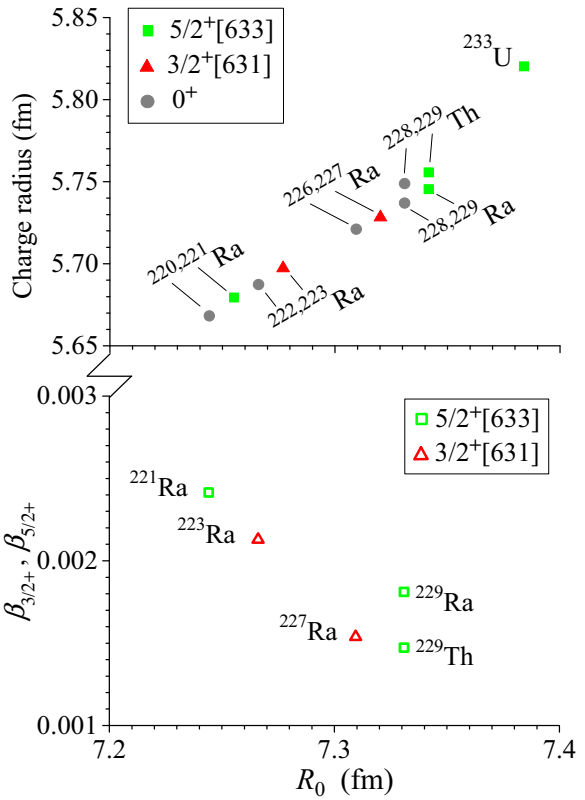

FIG. 3. Upper panel. The mean-square charge radii (a) of the even-even nuclei with the atomic number A and the spin 0^+, and (b) the related $A+1$ nuclei with the same Z and unpaired neutron in the ground states $5/2^+[633]$ and $3/2^+[631]$ (data from Ref. [59].) Lower panel: The quantities $\beta_{3/2^+}$ and $\beta_{5/2^+}$, Eq. (16).

Let us now consider the change of the mean-square charge radius of the even-even nuclei with the spin 0^+ when one neutron is added to the states $5/2^+[633]$ and $3/2^+[631]$

$$\frac{d\langle R^2\rangle_{A\to A+1}}{dA} \equiv \langle R^2\rangle_{3/2^+(5/2^+)} - \langle R^2\rangle_{0^+}. \qquad (15)$$

(Notice that in Eqs. (15)–(16) the nucleus with the atomic number A has the spin 0^+ and the mean-square charge radius $\langle R^2\rangle_{0^+}$. The nuclei with the atomic number $A+1$ have the spins $3/2^+$ or $5/2^+$ and the mean-square charge radii $\langle R^2\rangle_{3/2^+}$ or $\langle R^2\rangle_{5/2^+}$, respectively.)

In Fig. 3 we plot the quantities

$$\beta_{3/2^+(5/2^+)} = \frac{d\langle R^2\rangle_{A\to A+1}}{dA}\frac{1}{R^2_{0_{3/2^+(5/2^+)}}}, \qquad (16)$$

obtained on the basis of the data from Ref. [59]. (The choice of $\beta_{3/2^+(5/2^+)}$ will be justified below.) It can be seen that for $A = 229$ the characteristic values of $\beta_{3/2^+(5/2^+)}$ are in the range 0–0.003. Therefore, we are led to the relation $0 \leqslant |\beta_{3/2^+} - \beta_{5/2^+}| \leqslant 3\times 10^{-3}$. Since it is impossible to predict the value of $\beta_{3/2^+} - \beta_{5/2^+}$ more precisely using the available data, below we assume that $\beta_{3/2^+} - \beta_{5/2^+} \simeq 10^{-3}$.

Notice that with the quantities $\beta_{3/2^+(5/2^+)}$ introduced in Eqs. (15) to (16) we have the following relation

$$\langle R^2\rangle_{3/2^+} - \langle R^2\rangle_{5/2^+} = R^2_{0_{A=229}}(\beta_{3/2^+} - \beta_{5/2^+}) \qquad (17)$$

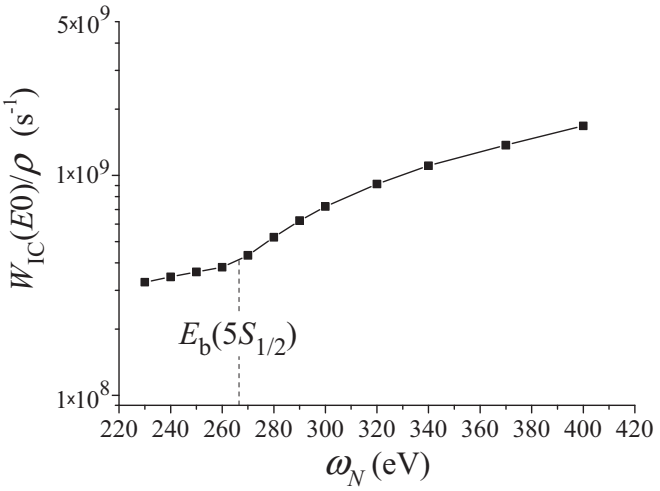

FIG. 4. The total electronic factor Ω_{tot} as the function of the energy of the $E0$ transition.

for the ^{229}Th nucleus. Equation (17) now can be substituted in Eq. (14). (As will be shown below, the difference $\beta_{3/2^+} - \beta_{5/2^+}$ coincides with the standard nuclear matrix element, used in the theory of the $E0$ transitions.)

V. NUMERICAL ESTIMATIONS AND DISCUSSION

Taking into account obtained estimation for the nuclear part and the data of Table I for the electron part we calculated the internal conversion probability in the muonic atom $(\mu^-_{1S_{1/2}}{}^{229}\mathrm{Th})^*$ and obtained $W_{E0}(370\,\mathrm{eV}) = 1.6 \times 10^{-13}$ eV. Correspondingly, the boundary values of W_{E0} are $W_{E0}(400\,\mathrm{eV}) = 1.9 \times 10^{-13}$ eV, and $W_{E0}(320\,\mathrm{eV}) = 3.7 \times 10^{-14}$ eV.

The graph of the total electronic factor

$$\Omega_{tot} = W_{E0}/[b^2(1-b^2)(\beta_{3/2^+} - \beta_{5/2^+})^2]$$

is represented in Fig. 4 for the entire range of the $E0$ energy uncertainty. The increase in the probability of the internal conversion for $\omega_N > 266$ eV is due to the inclusion of the $5S_{1/2}$ shell.

The calculated values for W_{E0} are significantly lower than the total width of the $M1$ transition in Fig. 1: $W_{M1}^{\gamma+IC} \simeq 7 \times 10^{-7}$ eV [43]. Such a small probability of the $E0$ transition is accounted for by the very small difference $\beta_{3/2^+} - \beta_{5/2^+}$. Let us consider this question in more detail.

From Eq. (17) one can see that the matrix element of the nuclear $E0$ transition $3/2^+ \to 5/2^+$ in ^{229}Th

$$\rho(E0; 3/2^+ \to 5/2^+) \equiv \beta_{3/2^+} - \beta_{5/2^+} = \frac{\langle R^2\rangle_{3/2^+} - \langle R^2\rangle_{5/2^+}}{R^2_{0_{A=229}}} \quad (18)$$

is an analog (up to the factor $b\sqrt{1-b^2}$) of the nuclear matrix element ρ_{fi}

$$\rho_{fi}(E0) = \frac{\langle f|\sum_k e_k R_k^2|i\rangle}{eR_0^2}, \quad (19)$$

the well known in the theory of $E0$ transitions [47]. Note that ρ_{fi} containing the nuclear structure information describes the strength of the $E0$ transition.

Typical values of ρ^2_{fi} given in Ref. [47] are $10^{-1} - 10^{-3}$ for the $0^+ \to 0^+$ and $2^+ \to 2^+$ transitions. This is 3 to 5 orders of magnitude greater than the value of $\rho^2(E0; 3/2^+ \to 5/2^+)$ for the ^{229}Th nucleus. However, as we already noted, usually $E0$ transitions occur between the nuclear levels whose energies differ by hundreds keV to several MeV. Consequently, the shape and charge radius of the nucleus in such states may strongly differ from one another.

The situation is very different for the ^{229}Th nucleus. The low-lying isomeric state and the ground state are practically degenerate in energy. They have fairly close configurations in the quantum numbers of the Nilsson model, and are connected with each other by the weakly forbidden $M1$ transition. As a consequence, the shapes of the ^{229}Th nucleus in these states and the mean-square charge radii are probably very close. This view is supported by the mean-square charge radii of the Ra nuclei in the $3/2^+[631]$ and $5/2^+[633]$ ground states shown in Fig. 3. Thus, the estimate $W_{E0} \simeq 10^{-13}$ eV obtained for the probability of the $E0$ transition in ^{229}Th looks conceivable. However, the final answer can be given only by the experiment.

VI. CONCLUSION

In conclusion, we derived formulas and obtained numerical estimates for the probability of the $E0$ transition between components of the magnetic hyperfine structure of the ground-state doublet in the muonic atom ^{229}Th. The mean-square charge radius of the ^{229}Th nucleus in the $3/2^+(7.8$ eV) state and the nuclear matrix element of the $E0$ transition $3/2^+(7.8\,\mathrm{eV}) \to 5/2^+(0.0)$ were estimated from the experimental data for the mean-square charge radii of the Ra nuclei. The electron wave functions in the bound and continuum states, as well as the electronic matrix elements have been calculated using the atomic computer codes [11,55–58], well-proven in the calculations of the internal conversion. The anomalously low probability of the $E0$ transition in the muonic atom $(\mu^-_{1S_{1/2}}{}^{229}\mathrm{Th})^*$ can be explained by a very small difference between the mean-square charge radii of the states of the ^{229}Th ground-state doublet.

ACKNOWLEDGMENTS

The author is grateful to Professor A.V. Nikolaev for the calculation of the electron wave functions in the Ac atom by the code [57,58]. This research was supported by a grant of the Russian Science Foundation (Project No. 16-12-00001).

[1] B. R. Beck, J. A. Becker, P. Beiersdorfer, G. V. Brown, K. J. Moody, J. B. Wilhelmy, F. S. Porter, C. A. Kilbourne, and R. L. Kelley, Phys. Rev. Lett. **98**, 142501 (2007).

[2] B. R. Beck, J. A. Becker, P. Beiersdorfer, G. V. Brown, K. J. Moody, J. B. Wilhelmy, F. S. Porter, C. A. Kilbourne, and R. L. Kelley, Report No. LLNL-PROC-415170.

[3] C. W. Reich and R. G. Helmer, Phys. Rev. Lett. **64**, 271 (1990).
[4] R. G. Helmer and C. W. Reich, Phys. Rev. C **49**, 1845 (1994).
[5] L. von der Wense *et al.*, Nature (London) **533**, 47 (2016).
[6] J. Jeet, C. Schneider, S. T. Sullivan, W. G. Rellergert, S. Mirzadeh, A. Cassanho, H. P. Jenssen, E. V. Tkalya, and E. R. Hudson, Phys. Rev. Lett. **114**, 253001 (2015).
[7] E. V. Tkalya, C. Schneider, J. Jeet, and E. R. Hudson, Phys. Rev. C **92**, 054324 (2015).
[8] R. H. Dicke, Phys. Rev. **93**, 99 (1954).
[9] E. V. Tkalya, JETP Lett. **71**, 311 (2000).
[10] E. V. Tkalya, A. N. Zherikhin, and V. I. Zhudov, Phys. Rev. C **61**, 064308 (2000).
[11] V. F. Strizhov and E. V. Tkalya, Sov. Phys. JETP **72**, 387 (1991).
[12] S. G. Porsev and V. V. Flambaum, Phys. Rev. A **81**, 032504 (2010).
[13] S. G. Porsev and V. V. Flambaum, Phys. Rev. A **81**, 042516 (2010).
[14] A. M. Dykhne, N. V. Eremin, and E. V. Tkalya, JETP Lett. **64**, 345 (1996).
[15] E. V. Tkalya, Phys. Rev. Lett. **106**, 162501 (2011).
[16] J. C. Berengut, V. A. Dzuba, V. V. Flambaum, and S. G. Porsev, Phys. Rev. Lett. **102**, 210801 (2009).
[17] V. V. Flambaum, Phys. Rev. Lett. **97**, 092502 (2006).
[18] H.-T. He and Z.-Z. Ren, J. Phys. G: Nucl. Phys. **34**, 1611 (2007).
[19] A. Hayes and J. Friar, Phys. Lett. B **650**, 229 (2007).
[20] E. Litvinova, H. Feldmeier, J. Dobaczewski, and V. Flambaum, Phys. Rev. C **79**, 064303 (2009).
[21] A. M. Dykhne and E. V. Tkalya, JETP Lett. **67**, 549 (1998).
[22] E. Peik and C. Tamm, Europhys. Lett. **61**, 181 (2000).
[23] W. G. Rellergert, D. DeMille, R. R. Greco, M. P. Hehlen, J. R. Torgerson, and E. R. Hudson, Phys. Rev. Lett. **104**, 200802 (2010).
[24] C. J. Campbell, A. G. Radnaev, A. Kuzmich, V. A. Dzuba, V. V. Flambaum, and A. Derevianko, Phys. Rev. Lett. **108**, 120802 (2012).
[25] E. Peik and M. Okhapkin, C. R. Phys. **16**, 516 (2015).
[26] E. V. Tkalya and L. P. Yatsenko, Laser Phys. Lett. **10**, 105808 (2013).
[27] M. P. Hehlen, R. R. Greco, W. G. Rellergert, S. T. Sullivan, D. DeMille, R. A. Jackson, E. R. Hudson, and J. R. Torgerson, J. Lumin. **133**, 91 (2013).
[28] S. Stellmer, M. Schreitl, and T. Schumm, Sci. Rep. **5**, 15580 (2015).
[29] G. Kazakov, V. Schauer, J. Schwestka, S. Stellmer, J. Sterba, A. Fleischmann, L. Gastaldo, A. Pabinger, C. Enss, and T. Schumm, Nucl. Instrum. Methods Phys. Res., Sect. A **735**, 229 (2014).
[30] P. Dessovic, P. Mohn, R. Jackson, G. Winkler, M. Schreit, G. Kazakov, and T. Schumm, J. Phys.: Condens. Matter **26**, 105402 (2014).
[31] A. Yamaguchi, M. Kolbe, H. Kaser, T. Reichel, A. Gottwald, and E. Peik, New J. Phys. **17**, 053053 (2015).
[32] M. V. Okhapkin, D. M. Meier, E. Peik, M. S. Safronova, M. G. Kozlov, and S. G. Porsev, Phys. Rev. A **92**, 020503(R) (2015).
[33] C. J. Campbell, A. G. Radnaev, and A. Kuzmich, Phys. Rev. Lett. **106**, 223001 (2011).
[34] A. M. Dykhne and E. V. Tkalya, JETP Lett. **67**, 251 (1998).
[35] J. C. E. Bemis, F. K. McGowan, J. J. L. C. Ford, W. T. Milner, R. L. Robinson, P. H. Stelson, G. A. Leander, and C. W. Reich, Phys. Scr. **38**, 657 (1988).
[36] A. Dupays, A. Beswick, B. Lepetit, C. Rizzo, and D. Bakalov, Phys. Rev. A **68**, 052503 (2003).
[37] R. Pohl *et al.*, Nature (London) **466**, 213 (2010).
[38] A. Adamczak, D. Bakalov, L. Stoychev, and A. Vacchi, Nucl. Instrum. Methods Phys. Res., Sect. B **281**, 72 (2012).
[39] A. Antognini *et al.*, Science **339**, 417 (2013).
[40] M. Sato *et al.*, JPS Conf. Proc. **8**, 025005 (2015).
[41] D. Guffanti on behalf of the FAMU collaboration, J. Phys.: Conf. Ser. **689**, 012018 (2016).
[42] R. Pohl *et al.*, Science **353**, 669 (2016).
[43] E. V. Tkalya, Phys. Rev. A **94**, 012510 (2016).
[44] S. Wycech and J. Zylicz, Acta Phys. Pol. B **24**, 637 (1993).
[45] K. Heyde and J. Wood, Rev. Mod. Phys. **83**, 1467 (2011).
[46] S. G. Nilsson, Mat.-Fys Medd. Danske Selskab **Bd. 29**, n. 16 (1955).
[47] J. Wood, E. Zganjar, C. D. Coster, and K. Heyde, Nucl. Phys. A **651**, 323 (1999).
[48] R. Hager and E. Seltzer, Nucl. Data Tables **6**, 1 (1969).
[49] D. Bell, C. Aveledo, M. Davidson, and J. Davidson, Can. J. Phys. **48**, 2542 (1970).
[50] J. Kantele, Nucl. Instrum. Methods Phys. Res., Sect. A **271**, 625 (1988).
[51] E. L. Church and J. Weneser, Phys. Rev. **104**, 1382 (1956).
[52] A. Bohr and V. F. Weisskopf, Phys. Rev. **77**, 94 (1950).
[53] E. V. Tkalya, JETP **78**, 239 (1994).
[54] E. L. Church and J. Weneser, Annu. Rev. Nucl. Sci. **10**, 193 (1960).
[55] A. A. Soldatov and D. P. Grechukhin, Kourchatov Institute of Atomic Energy Report No. 3174, Moscow, 1979.
[56] I. M. Band and V. I. Fomichev, At. Data Nucl. Data Tables **23**, 295 (1979).
[57] A. Nikolaev, D. Lamoen, and B. Partoens., J. Chem. Phys. **145**, 014101 (2016).
[58] A. V. Nikolaev, The FLAPW-Moscow code [registration number 2015616990 (Russia) from 26/06/2015].
[59] I. Angeli and K. Marinova, At. Data Nucl. Data Tables **99**, 69 (2013).